

Linear Optimal Power Flow Using Cycle Flows

Jonas Hörsch^a, Henrik Ronellenfitsch^b, Dirk Witthaut^{c,d}, Tom Brown^{a,*}

^aFrankfurt Institute for Advanced Studies, 60438 Frankfurt am Main, Germany

^bDepartment of Physics and Astronomy, University of Pennsylvania, Philadelphia PA, USA

^cForschungszentrum Jülich, Institute for Energy and Climate Research - Systems Analysis and Technology Evaluation (IEK-STE), 52428 Jülich, Germany

^dInstitute for Theoretical Physics, University of Cologne, 50937 Köln, Germany

Abstract

Linear optimal power flow (LOPF) algorithms use a linearization of the alternating current (AC) load flow equations to optimize generator dispatch in a network subject to the loading constraints of the network branches. Common algorithms use the voltage angles at the buses as optimization variables, but alternatives can be computationally advantageous. In this article we provide a review of existing methods and describe new formulations, which express the loading constraints directly in terms of the flows themselves, using a decomposition of the network graph into a spanning tree and closed cycles. We provide a comprehensive study of the computational performance of the various formulations, in settings that include computationally challenging applications such as multi-period LOPF with storage dispatch and generation capacity expansion. We show that one of the new formulations of the LOPF solves up to 20 times faster than the angle formulation using commercial linear programming solvers, with an average speed-up of factor 3 for the standard networks considered here. If generation capacities are also optimized, the average speed-up rises to a factor of 12, reaching up to factor 213 in a particular instance. The speed-up is largest for networks with many buses and decentral generators throughout the network, which is highly relevant given the rise of distributed renewable generation and the computational challenge of operation and planning in such networks.

Keywords: Linear Optimal Power Flow, DC power flow, dual network, graph theory

1. Introduction

Optimal Power Flow (OPF) problems can be constructed to find the welfare-maximizing generation and consumption levels in a network given the physical load flow equations, branch loading limits and generator cost functions. The full load flow equations are non-linear and the resulting optimization problem is non-convex, which makes it both challenging and computationally expensive to find a global optimum [1]. In transmission networks with sufficient reactive power compensation, linearizing the load flow equations introduces only small errors [2, 3], with the benefit that the Linear OPF (LOPF) can be expressed as a linear problem, whose convexity guarantees that a local optimum is a global optimum.

LOPF algorithms are principally used in applications with high computational complexity where it would be impossible to use the full load flow equations, such as clearing markets with nodal pricing [4] (particularly with multi-period storage constraints and/or generator unit commitment), determining re-dispatch measures in markets with zonal pricing [5], optimizing dispatch taking account of contingencies (Security Constrained LOPF (SCLOPF)) [6, 7] and in the long-term optimization of investment in generation and transmission assets [8, 9]. Where higher accuracy solutions are required, linear solutions can be

fed as an initial solution into algorithms that use the full non-linear load flow equations [1]. LOPF is becoming more important with the growth of renewable energy, since the fluctuating feed-in has led to more frequent situations where the network is highly loaded [10]. When large networks are optimized over multiple representative feed-in situations, especially with discrete constraints on generation dispatch, the LOPF problems can still take a significant time to solve, despite the linearization of the problem. Approaches in the literature to reducing the computational times of LOPF problems include decomposition [11, 12, 13, 14, 15], reformulating the problem using Power Transfer Distribution Factors (PTDFs) [16, 17] and a parallelizable algorithm using the primal-dual interior point method [18].

In textbooks [6, 19] and major software packages such as MATPOWER [20], DIgSILENT PowerFactory [21], PowerWorld [22] and PSAT [23], the linearization of the relations between power flows in the network and power injection at the buses is expressed indirectly through auxiliary variables that represent the voltage angles at the buses. In this paper we introduce two new formulations of the linear equations that use the power flows directly, decomposed using graph theoretic techniques into flows on a spanning tree and flows around closed cycles in the network. We evaluate the computational performance of the various methods for the LOPF problem, showing that the new formulations can solve significantly faster than the traditional angle-based formulation. We examine not just the basic LOPF problem, but also applications that include more

*Corresponding author

Email address: brown@fias.uni-frankfurt.de (Tom Brown)

Table 1: Variable definitions

Variable	Definition
$i, j \in \{1, \dots, N\}$	Bus labels
$s \in \{1, \dots, G\}$	Generation source labels (wind, solar, gas, etc.)
$k, \ell \in \{1, \dots, L\}$	Branch labels
$c, d \in \{1, \dots, L - N + 1\}$	Cycle labels
$t \in \{1, \dots, T\}$	Snapshot / time point labels
$d_{i,s}$	Dispatch of generator at bus i with source s
$D_{i,s}$	Available power of generator i, s
l_i	Electrical load at bus i
θ_i	Voltage angle at bus i
p_i	Total active power injection
θ_ℓ	Voltage angle across a branch
f_ℓ	Branch active power flow
g_ℓ	Flow on spanning tree (zero if ℓ not in tree)
h_c	Flow around cycle c
F_ℓ	Branch active power rating
x_ℓ	Branch series reactance
$K_{i\ell}$	$N \times L$ incidence matrix
$C_{\ell c}$	$L \times (L - N + 1)$ cycle matrix
$T_{\ell i}$	$L \times N$ tree matrix
$B_{\ell k}$	Diagonal $L \times L$ matrix of branch susceptances
Λ	$N \times N$ weighted Laplacian matrix $\Lambda = KBK^T$

computationally challenging multi-period storage optimization and generation capacity expansion.

Cycle-flow techniques have already been used in [24] to improve the calculation times of PTDFs and to gain a new understanding of the propagation of line outages in networks [25]. While preparing this manuscript, another paper [26] using cycle flows for single-period LOPF with optimal transmission switching was published; in contrast to that paper, here we provide an additional new formulation and benchmark both formulations against established formulations for a different set of computationally-challenging problems: those extending over multiple periods.

In Section 2 the different formulations of the linear load flow are reviewed to prepare for the introduction of the optimization in Section 3. Extensions beyond the basic LOPF problem are described in Section 4 and the results of the performance analysis are presented in Section 5.

2. Linear load flow formulations

The aim of the linear load flow calculation is to calculate the active power flow f_ℓ on each of the branches $\ell = 1, \dots, L$ in terms of the active power p_i injected or consumed at each of the buses $i = 1, \dots, N$. In this section four methods are presented for solving the linear load flow, which lead to different formulations of the LOPF problem discussed below.

The linear approximation is valid if all branch resistances r_ℓ are negligible compared to the branch reactances x_ℓ , $r_\ell \ll |x_\ell|$,

reactive power flows may be neglected, all voltage magnitudes are kept at nominal value and if all voltage angle differences across branches θ_ℓ are small enough that we can approximate $\sin \theta_\ell \sim \theta_\ell$ [2, 3]. Then the real power over a transmission line ℓ is given by

$$f_\ell = \frac{\theta_\ell}{x_\ell}, \quad (1)$$

where θ_ℓ is the voltage angle difference between the terminal buses of line ℓ .

The flows f_ℓ are constrained to be physical by the two Kirchhoff circuit laws for the current and voltage. Kirchhoff's Current Law (KCL) states that the current injected at each bus must equal the current withdrawn by the branches attached to the bus. This law can be expressed using the incidence matrix $K_{i\ell}$, which has non-zero values $+1$ if branch ℓ starts on bus i and -1 if branch ℓ ends on bus i . KCL then reads

$$p_i = \sum_{\ell} K_{i\ell} f_\ell \quad \forall i = 1, \dots, N. \quad (2)$$

KCL directly implies power conservation $\sum_i p_i = 0$ because $\sum_i K_{i\ell} = 0$ for all lines ℓ . KCL provides N linear equations for the L unknown flows f_ℓ , of which one is linearly dependent. This is not sufficient to uniquely determine the flows unless the network is a tree. Hence, $L - N + 1$ additional independent equations are needed.

The necessary equations and physicality are provided by the Kirchhoff Voltage Law (KVL), which states that the sum of potential differences across branches around all cycles in the network must sum to zero. It follows from graph theory that there are $L - N + 1$ independent cycles for a connected graph [27], which provides enough equations to constrain the f_ℓ completely. The independent cycles $c \in \{1, \dots, L - N + 1\}$ are expressed as a directed linear combination of the branches ℓ in the cycle incidence matrix

$$C_{\ell c} = \begin{cases} 1 & \text{if edge } \ell \text{ is element of cycle } c, \\ -1 & \text{if reversed edge } \ell \text{ is element of cycle } c, \\ 0 & \text{otherwise.} \end{cases} \quad (3)$$

Then the KVL becomes

$$\sum_{\ell} C_{\ell c} \theta_\ell = 0 \quad \forall c = 1, \dots, L - N + 1. \quad (4)$$

where $\theta_\ell = \theta_i - \theta_j$ is the angle difference between the two buses i, j which branch ℓ connects. Using equation (2), KVL can be expressed in terms of the power flows as

$$\sum_{\ell} C_{\ell c} x_\ell f_\ell = 0 \quad \forall c = 1, \dots, L - N + 1. \quad (5)$$

2.1. Angle formulation

Commonly, the linear load flow problem is formulated in terms of the voltage phase angles $\theta_i, i \in \{1, \dots, N\}$. Using the incidence matrix the power flows are expressed as

$$f_\ell = \frac{1}{x_\ell} \sum_i K_{i\ell} \theta_i \quad \forall \ell = 1, \dots, L \quad (6)$$

If the $L \times L$ diagonal matrix B is defined with $B_{\ell\ell} = \frac{1}{x_\ell}$ then the KCL equation (2) becomes

$$\begin{aligned} p_i &= \sum_{\ell,k,j} K_{i\ell} B_{\ell\ell} K_{jk} \theta_j \\ &= \sum_j \Lambda_{ij} \theta_j, \quad \forall i = 1, \dots, N, \end{aligned} \quad (7)$$

using the nodal susceptance matrix matrix $\Lambda = KBK^T$. In mathematical terms, Λ is a weighted network Laplacian [28].

The Angle formulation thus consists of two consecutive steps to calculate the flows f_ℓ . First, equation (7) is solved to obtain the N voltage angles θ_i . The equation provides only $N - 1$ independent conditions such that we typically fix the voltage angle at a slack bus as $\theta_0 = 0$. Second, the flows are calculated via Equation (6). KVL is automatically satisfied as all closed cycles are in the kernel of the incidence matrix such that

$$\sum_\ell K_{i\ell} C_{\ell c} = 0 \quad \forall c = 1, \dots, L - N + 1. \quad (8)$$

2.2. PTDF formulation

For the Power Transfer Distribution Factor (PTDF) formulation [6] the matrix defining equation (7) is explicitly inverted to get the angles in terms of the power injections, and the resulting expression for the angles inserted into (6) to get a direct linear relation:

$$f_\ell = \sum_i PTDF_{\ell i} p_i \quad \forall \ell = 1, \dots, L, \quad (9)$$

where the PTDF matrix is given by $PTDF = BK^T \Lambda^*$. The pseudo-inverse Λ^* is used because Λ contains a zero eigenvalue for a connected network. Because KCL is no longer explicitly enforced, power conservation $\sum_i p_i = 0$ must be added as an explicit constraint for each connected network. The need to calculate the explicit pseudo-inverse of Λ makes this slow compared to the Angle formulation for single calculations, but once the PTDF has been computed, repeated application involves only matrix multiplication and no equation-solving. However, the PTDF matrix is typically dense, while Λ and K are sparse.

2.3. Kirchhoff formulation

In what we call the ‘Kirchhoff formulation’, the linear load flow is expressed as explicit linear constraints on the flows themselves. To the $N - 1$ independent equations of the KCL equation from (2) we add the $L - N + 1$ constraints of the KVL from (5). Together, this provides a system of L independent equations for the L variables f_ℓ and can therefore be solved.

2.4. Cycle formulation

In what we call the ‘Cycle formulation’ the flows f_ℓ are decomposed into a superposition of the flows g_ℓ on a spanning tree of the network, which ensure KCL is satisfied, and into cycle flows h_c that flow around each independent cycle c in the network without altering the power balance at any bus [24]. We thus have:

$$f_\ell = g_\ell + \sum_c C_{\ell c} h_c. \quad (10)$$

The g_ℓ are only non-zero on the $N - 1$ edges of a chosen spanning tree of the connected network. They are uniquely determined from the power imbalances by a matrix T

$$g_\ell = \sum_i T_{\ell i} p_i. \quad (11)$$

T is determined by fixing a slack bus and giving $T_{\ell i}$ value +1 if branch ℓ is in the directed path in the spanning tree from i to the slack bus or -1 if it is in the directed path but with reversed orientation [24]. This guarantees that KCL is satisfied at every bus given that the power is balanced, $\sum_i p_i = 0$. Note that T only has to be calculated once for a network and is independent of the p_i . There is freedom both in the choice of spanning tree and in the choice of the slack bus used to determine the matrix T .

The remaining $L - N + 1$ degrees of freedom for the cycle flows h_c are fixed by the $L - N + 1$ additional constraints from KVL (5)

$$\sum_\ell C_{\ell c} x_\ell \left(g_\ell + \sum_d C_{\ell d} h_d \right) = 0 \quad \forall c \quad (12)$$

Solving this equation for the h_c involves solving $L - N + 1$ linear equations. Power networks are not so heavily meshed, typically $L - N + 1 < N - 1$, such that this method can be significantly faster than the Angle formulation [24, 25].

3. Linear optimal power flow formulations

In this section the linear load flow methods from Section 2 are transposed to the linear optimal power flow (LOPF). In optimal power flow, power plant dispatch is optimized to minimize dispatch costs, assuming that no branch flows f_ℓ exceed their loading limits F_ℓ , i.e. $|f_\ell| \leq F_\ell$ [6].

The factors which control the speed of the solution to the LOPF problem are now more subtle. They include: i) the number of optimization variables; ii) the number of constraints; iii) the sparsity or density of the constraint matrix; iv) the shape of the feasible space near the optimal point; v) the method used to solve the linear problem. The first three factors are summarized for each of the formulations in Table 2.

The objective function for the LOPF has the generic form

$$\min_{\{d_{i,s}, \{z_a\}\}} \left[\sum_{i,s} c_{i,s} d_{i,s} \right] \quad (13)$$

where $d_{i,s}$ is the dispatch of generator s at bus i and $c_{i,s}$ is its operating cost. The z_a are auxiliary variables that implement the network constraints and depend on the problem formulation (for instance, they would be the voltage angles in the case of the Angle formulation).

One can also include the line flows f_ℓ as explicit optimization variables. The generic optimization problem then reads

$$\min_{\{d_{i,s}, \{z_a\}, \{f_\ell\}\}} \left[\sum_{i,s} c_{i,s} d_{i,s} \right] \quad (14)$$

All variables and their definitions are listed in Table 1.

Table 2: Overview of the different formulations of the LOPF problem (N : number of buses, L : number of transmission lines, G : number of dispatchable generators)

Formulation	Variables	# Variables	# Equality constraints	# Inequality constraints	Matrices
Pure Angle	$d_{i,s}, \theta_i$	$G + N$	$N + 1$	$G + 2L$	sparse
Angle+Flow	$d_{i,s}, f_\ell, \theta_i$	$G + L + N$	$L + N + 1$	$G + 2L$	sparse
Pure PTDF	$d_{i,s}$	G	1	$G + 2L$	dense
PTDF+Flow	$d_{i,s}, f_\ell$	$G + L$	$L + 1$	$G + 2L$	dense
Kirchhoff	$d_{i,s}, f_\ell$	$G + L$	$L + 1$	$G + 2L$	sparse
Pure Cycle	$d_{i,s}, h_c$	$G + L - N + 1$	$L - N + 2$	$G + 2L$	semi-sparse
Cycle+Flow	$d_{i,s}, h_c, f_\ell$	$G + 2L - N + 1$	$2L - N + 2$	$G + 2L$	semi-sparse

The optimization must respect several constraints. First, the load l_i at each bus (which is assumed to be inelastic) must always be met. The bus power balance is the difference between generation and the electrical load l_i at the bus

$$p_i = \sum_s d_{is} - l_i. \quad (15)$$

If $p_i > 0$ then the bus is a net exporter of power; if $p_i < 0$ then the bus is a net importer of power. Note that p_i is only used to organize the presentation of the equations and is not an explicit optimization variable. Second, each generator must dispatch within its available power

$$0 \leq d_{i,s} \leq D_{i,s} \quad \forall \text{ generators}. \quad (16)$$

Third, the real power flows must remain within the loading limits of the lines

$$|f_\ell| \leq F_\ell \quad \forall \ell = 1, \dots, L. \quad (17)$$

It is sometimes desirable to limit the magnitude of the voltage angle differences θ_ℓ across the branches, to maintain the $\sin \theta_\ell \sim \theta_\ell$ approximation and avoid voltage stability problems [29]. Since $\theta_\ell = x_\ell f_\ell$, this constraint has the same form as the loading limit constraint (17), so we do not consider it further. Note that the load at each bus l_i , specific costs $c_{i,s}$, generation upper limits $D_{i,s}$, branch loading limits F_ℓ and branch reactances x_ℓ are all exogenous data inputs and not subject to optimization in the considerations here. In all cases here the network is assumed to be connected and only a single time point is considered. Extensions are discussed in the next section.

Finally active power flows on each branch f_ℓ are determined by the p_i and the auxiliary variables z_a through the constraints

$$f_\ell \equiv f_\ell(p_i, z_a) \quad (18)$$

The different formulations of the network equations presented in Section 2 give rise to different formulations of the linear OPF. Whether we include the flows f_ℓ and additional auxiliary variables z_a as optimization variables has a significant impact on the computational resources needed to solve the optimization task. In the following we specify the different formulations of the linear OPF (LOPF) in detail; their properties are summarized in Table 2. Note that for a uniquely-defined problem, all the formulations deliver the same optimum.

3.1. Pure Angle formulation

In the Pure Angle formulation the optimization problem (13) is solved with the voltage angles as auxiliary variables $\{z_a\} = \{\theta_i\}$ subject to the constraints (16) and

$$\begin{aligned} \left| \sum_i (BK^T)_{\ell i} \theta_i \right| &\leq F_\ell & \forall \ell = 1, \dots, L, \\ p_i &= \sum_j \Lambda_j \theta_j & \forall i = 1, \dots, N, \\ \theta_0 &= 0. \end{aligned} \quad (19)$$

The first equation ensures no branch overloading (note that it is sparse, inheriting the sparsity of K), the second equation is KCL and in the final equation the phase angle is fixed at the reference bus, which removes an unnecessary degree of freedom. Here and in the following the p_i are used as a short-hand notation according to equation (15).

The Pure Angle formulation is used in the free software tools MATPOWER [20] and PYPOWER [30]; it is therefore used as the benchmark implementation against which we compare all other formulations in Section 5.

3.2. Angle+Flow formulation

For the Angle+Flow formulation of the LOPF the flows f_ℓ are introduced as explicit optimization variables and the voltage angles are retained as auxiliary variables. Hence we have to solve the optimization problem (14) with N auxiliary variables, $\{z_a\} = \{\theta_i\}$ subject to the constraints (17) and (16) and the network equations

$$\begin{aligned} f_\ell &= \sum_i (BK^T)_{\ell i} \theta_i & \forall \ell = 1, \dots, L, \\ p_i &= \sum_\ell K_{i\ell} f_\ell & \forall i = 1, \dots, N, \\ \theta_0 &= 0. \end{aligned} \quad (20)$$

The introduction of additional optimization variables f_ℓ might appear to be redundant and unnecessary, but it will be shown to cause a significant speed-up in some cases. This is because modern solvers have sophisticated algorithms to ‘pre-solve’ solutions and remove redundancy that may not be obvious.

3.3. Pure PTDF formulation

In the Pure PTDF formulation no auxiliary variables are used such that the optimization problem is given by (13) subject to the constraints (16) and

$$\begin{aligned} \left| \sum_i PTDF_{\ell,i} p_i \right| &\leq F_\ell \quad \forall \ell = 1, \dots, L, \\ \sum_i p_i &= 0. \end{aligned} \quad (21)$$

This formulation minimizes the number of optimization variables, but suffers from the fact that the matrix $PTDF$ is dense. This generates a large number of dense inequalities, which can be slow to process for large problems and may make the feasible space complicated by introducing lots of interdependencies between the variables. This formulation has been used in the literature in, for example, [31]. One advantage of this formulation is that the constraints are independent for each line, so that the constraints can also be limited to subsets of lines. This is useful when it is known in advance which lines are typically constraining.

3.4. PTDF+Flow formulation

The PTDF+Flow formulation does not use any auxiliary variables, but keeps the flows as explicit optimization variables. Hence we have to solve the optimization problem (14) subject to the constraints (17) and (16) and the network equations

$$\begin{aligned} f_\ell &= \sum_i PTDF_{\ell,i} p_i \quad \forall \ell = 1, \dots, L, \\ \sum_i p_i &= 0. \end{aligned} \quad (22)$$

This formalism was used in [16, 17].

3.5. Kirchhoff formulation

The Kirchhoff formulation is a new formulation of the LOPF which only requires the flow variables f_ℓ and introduces no additional auxiliary variables. The optimization problem is given by (14) subject to the constraints (17) and (16) and the network equations

$$\begin{aligned} \sum_\ell K_{i\ell} f_\ell &= p_i \quad \forall \ell = 1, \dots, L, \\ \sum_\ell C_{\ell c} x_\ell f_\ell &= 0 \quad \forall c = 1, \dots, L - N + 1. \end{aligned} \quad (23)$$

This method implements the Kirchhoff circuit laws directly on the flow variables. It has both a small number of variables and extremely sparse constraints. As discussed in the introduction, this formulation was also introduced recently for optimal transmission switching [26].

3.6. Pure Cycle formulation

The Cycle formulation of the linear load flow problem introduced in Section (2.4) leads to new formulations of the LOPF. In the Pure Cycle formulation we solve the optimization problem (13) by adding $L - N + 1$ auxiliary variables $\{z_a\} = \{h_c\}$ subject to the constraints (16) and

$$\begin{aligned} \left| \sum_i T_{\ell i} p_i + \sum_c C_{\ell c} h_c \right| &\leq F_\ell \quad \forall \ell = 1, \dots, L, \\ \sum_\ell C_{\ell c} x_\ell \left[\sum_i T_{\ell i} p_i + \sum_{c'} C_{\ell c'} h_{c'} \right] &= 0 \\ &\quad \forall c = 1, \dots, L - N + 1, \\ \sum_i p_i &= 0. \end{aligned} \quad (24)$$

This involves fewer constraints than the Pure Angle formulation if $L < 2N$, which is typically true for power networks. However, because for some lines the matrix $T_{\ell i}$ may have many entries, the constraints can only be considered semi-sparse.

3.7. Cycle+Flow formulation

In the Cycle+Flow formulation we add auxiliary variables $\{z_a\} = \{h_c\}$ and include the flow variables f_ℓ as explicit optimization variables. The optimization problem is then given by (14) subject to the constraints (17) and (16) and the network equations

$$\begin{aligned} f_\ell &= \sum_i T_{\ell i} p_i + \sum_c C_{\ell c} h_c \quad \forall \ell = 1, \dots, L, \\ \sum_\ell C_{\ell c} x_\ell f_\ell &= 0 \quad \forall c = 1, \dots, L - N + 1, \\ \sum_i p_i &= 0. \end{aligned} \quad (25)$$

4. Extensions to LOPF

In this section we briefly sketch some extensions of the LOPF problem to related problems for which the methodology also applies.

4.1. Multi-period and stochastic optimization

Inter-temporal aspects of optimal power flow, such as the operation of storage units or power plant unit commitment, can be considered using multi-period OPF [6, 32]. For periods labeled t with weighting π_t the objective function becomes

$$\min_{\{d_{i,s,t}\}, \{z_{a,t}\}, \{f_{\ell,t}\}} \left[\sum_{i,s,t} \pi_t c_{i,s} d_{i,s,t} \right]. \quad (26)$$

The network flow constraints repeat for each period t .

Storage introduces inter-temporal constraints that ensure that the storage state of charge $soc_{i,s,t}$ stays below the maximum energy storage capacity $SOC_{i,s}$:

$$\begin{aligned} soc_{i,s,t} &= soc_{i,s,t-1} + \eta_1 d_{i,s,t,charge} - \eta_2^{-1} d_{i,s,t,discharge} \\ 0 &\leq soc_{i,s,t} \leq SOC_{i,s} \quad \forall i, s, t \end{aligned} \quad (27)$$

The efficiencies η_1, η_2 determine the losses during charging and discharging, respectively.

For stochastic optimization the periods t can represent different scenarios with probability π_t [32, 33, 34].

4.2. Generation investment optimization

For generation investment optimization, the power plant capacities $D_{i,s}$ are promoted from exogenous parameters to optimization variables with capital costs $C_{i,s}$ [32]. The objective function becomes

$$\min_{\{D_{i,s}\}, \{d_{i,s,t}\}, \{z_{a,t}\}, \{f_{\ell,t}\}} \left[\sum_{i,s} C_{i,s} D_{i,s} + \sum_{i,s,t} \pi_t c_{i,s} d_{i,s,t} \right].$$

The optimization is carried out over multiple periods t representing different demand and weather conditions, which makes such problems computationally challenging.

For investment optimization it is common to approximate the line outage contingency constraints by a blanket factor, e.g. limiting loading to 70% of thermal limits, to reduce the computationally complexity [9, 31, 35, 36].

4.3. Security-Constrained LOPF

In Security-Constrained LOPF (SCLOPF) line outages are modelled explicitly. It is required that no lines become overloaded if there is an outage of any branches in a critical subset [6].

SCLOPF can be implemented either by adding to the LOPF problem copies of all the network variables and constraints for networks without the critical branches, or by using Line Outage Distribution Factors (LODFs).

In the LODF formalism, for each branch k which is critical, the following set of constraints are added to the LOPF

$$|f_{\ell}^{(k)}| = |f_{\ell} + \text{LODF}_{\ell,k} f_k| \leq F_{\ell} \quad \forall \ell \neq k \quad (28)$$

Here f_{ℓ}, f_k are the flows before the outage and $f_{\ell}^{(k)}$ is the flow on ℓ after the outage of branch k . The flows before and after the outage are related linearly by the LODF matrix, which can also be computed efficiently using cycle flows [25].

In the first version of SCLOPF with copies of the network constraints with outages, it is expected that all the benefits of the cycle methods are preserved. In the LODF formalism the density of the LOPF matrix may blunt the benefits of a sparse formulation. The trade-offs between these issues will be examined in a forthcoming paper.

5. Results

In this section we compare the computational performance of the different formulations of the LOPF problem introduced in Section 3 for various different test grids. All LOPF formulations are implemented in ‘Python for Power System Analysis’ (PyPSA) [37], a free software tool developed at the Frankfurt Institute for Advanced Studies (FIAS). The formulation can be changed simply by passing a different argument ‘formulation’

to the LOPF function. PyPSA is used to generate linear program files (in CPLEX’s .lp format), which are then passed to a linear solver (here we use the commercial software Gurobi [38]). The solver is then run using different algorithms for the linear program (primal and dual simplex, interior point) and the total solving time averaged over multiple runs is compared. Only Gurobi’s solving time is presented, so that the results are independent of the program used to generate the optimization problem. The total solving time includes reading in the .lp file, pre-solving the matrix system and the solution algorithm. A computer system with 20 Intel Xeon E5-2650 cores @ 2.30GHz each and 128 GB RAM was used for each benchmark.

5.1. Problem preparation

Seven different network topologies are considered. case118, case300, case1354pegase, case1951rte, case2383wp and case2869pegase are taken from the MATPOWER software package [20] test cases (the IEEE standard cases as well as snapshots from the French TSO RTE and European networks [39]). In addition the open data SciGRID model of Germany’s transmission network [40] is also tested, which has 585 buses and 948 branches.

Only large networks were considered, because large problems represent the main target of efforts to improve computational speed. For the same reason, all networks were tested for multi-period optimization with 24 hours represented in each problem, which would be typical for short-term storage optimization or a unit commitment problem. Large problems also ensure that no small one-off delays can significantly affect the timing.

Each test grid only has a single snapshot of the load. This was extended to 24 hours by subtracting a small fraction of normally distributed random noise $\varepsilon \sim \mathcal{N}(0, 0.2)$

$$l_{i,t} = l_i (1 - |\varepsilon_{i,t}|), \quad (29)$$

to ensure that the problem remained feasible and the solver was unable to reduce the problem from 24 identical problems to a single one.

The configuration of the generation was varied in three different ‘modes’:

- p: (plain): Only the conventional generators of the model are available. There is no inter-temporal linkage between the snapshots.
- r: Compared to p, variable renewable generators are added to every single bus to represent decentralized generation. The time series of the power availability of the renewable generators are taken at random from wind and time series for Germany for the year 2011 generated using the Aarhus Renewable Energy Atlas [41]. The renewable generators may be curtailed such that they correspond to dispatchable generators with no variable costs. There is no inter-temporal linkage between the snapshots.
- rs: Compared to r, storage units with a power capacity of a third of the nodal mean load are added to the fifteen buses

Table 3: LOPF speed-up versus the Pure Angle formulation (> 1 means faster), best formulation marked green, worst marked red

mode	case	Avg. solution time (24 periods) Pure Angle [s]	Speed-up compared to Pure Angle					
			Angle+ Flow	Pure PTDF	PTDF+ Flow	Kirchhoff	Pure Cycle	Cycle+ Flow
p	case118	0.20	1.13	0.24	0.53	1.27	0.76	0.98
	case300	0.45	1.00	0.27	0.59	1.12	0.60	0.67
	case1354pegase	1.92	1.07	0.10	0.17	0.99	0.23	0.43
	case1951rte	3.21	0.22	0.14	0.27	1.30	0.32	0.55
	case2383wp	9.17	0.75	0.27	0.44	1.43	0.42	0.35
	case2869pegase	14.94	2.19	0.30	0.52	2.15	0.41	0.85
	scigrid	2.01	1.44	0.10	0.19	1.60	0.57	1.08
r	case118	0.25	0.99	0.12	0.23	1.22	0.58	0.88
	case300	0.77	1.12	0.11	0.20	1.37	0.54	0.73
	case1354pegase	7.58	1.38	0.06	0.10	2.55	0.42	0.87
	case1951rte	11.96	0.57	0.05	0.09	2.70	0.46	0.93
	case2383wp	65.17	3.40	0.13	0.24	4.31	1.13	1.55
	case2869pegase	51.83	0.83	0.06	0.10	3.60	0.43	1.18
	scigrid	3.60	1.62	0.06	0.12	2.44	0.75	1.14
rs	case118	0.26	0.99	0.13	0.23	1.24	0.61	0.90
	case300	0.77	1.11	0.11	0.19	1.38	0.55	0.73
	case1354pegase	7.45	1.35	0.06	0.10	2.42	0.42	0.89
	case1951rte	11.91	0.58	0.05	0.09	2.62	0.46	0.90
	case2383wp	60.73	3.22	0.14	0.25	4.12	1.10	1.44
	case2869pegase	52.88	0.85	0.07	0.11	3.61	0.45	1.20
	scigrid	7.26	2.70	0.12	0.25	4.14	1.33	2.03

with the highest average load. They provide an energy capacity of 6 hours at full power capacity and link the snapshots. More than 15 storage units made the computation times intractable.

For each network, mode and formulation, Gurobi was run in parallel using the primal simplex, the dual simplex and the interior point algorithms on at most four cores in parallel. The fastest solution was always taken. For each case and mode combination, 100 instances (i.e. different randomizations of the load and selections of the renewable time series) were generated and timed for all formulations except for the Pure PTDF and the PTDF+Flow formulations. For these only 10 instances were investigated, since the generation of a single of their lp files took up to 6 hours. The code for running the simulations with Snakemake [42] will be linked from the PyPSA website [43]. It was checked that all formulations gave identical results for the same problem, which is to be expected given that the formulations were shown in Sections 2 and 3 to be mathematically equivalent.

5.2. Comparing average speed-up of the different formulations

In Table 3 the speed-up for the different formulations of the LOPF for the different problems (averaged over 100 instances) are shown, compared to the standard Pure Angle formulation. The speed-up is defined by the time taken for the Pure Angle formulation divided by the time taken for the formulation in question. A speed-up over 1 means the formulation is faster.

The Kirchhoff formulation is the fastest in all cases where decentralized renewables are present in the network and the fastest

in all but two cases for the ‘plain’ mode, where the Angle+Flow formulation is faster by a small margin. For the Kirchhoff formulation the speed-up factor averages 1.4 in mode ‘p’, 2.6 in mode ‘r’ and 2.8 for mode ‘rs’. One reason the speed-up is high with renewables is that the optimization has to weigh up the dispatch at every single bus and their effects on the flows. A sparser, less interdependent constraint set is a bigger advantage than in mode ‘p’, where only a few buses have controllable generators. Inter-temporal storage introduces even more inter-dependences between variables, which again favours the sparse formulations.

The Angle+Flow formulation is the next fastest, averaging a speed improvement of 1.11 in mode ‘p’, 1.42 in mode ‘r’ and 1.54 in mode ‘rs’, despite the fact that there are more variables than the Pure Angle formulation.

The Cycle+Flow formulation is a factor 0.7 slower than the Pure Angle formulation in mode ‘p’, but faster by factor 1.04 in mode ‘r’ and 1.16 in mode ‘rs’. The Pure Cycle formulation is on average slower in all modes. In particular cases the Pure Cycle formulation is faster than Pure Angle, but in each of those cases Cycle+Flow is faster.

The PTDF methods are slowest of all, with the Pure PTDF being the slowest. This is primarily driven by the size of the linear programming problem file, which takes a long time to read in by the solver. The size of the file is driven by the dense constraints coming from the dense PTDF matrix. For large networks with many periods, the file sizes were many gigabytes, leading to problems writing them and storing them. Once the .lp problem is read in and pre-solved, the solving time is in

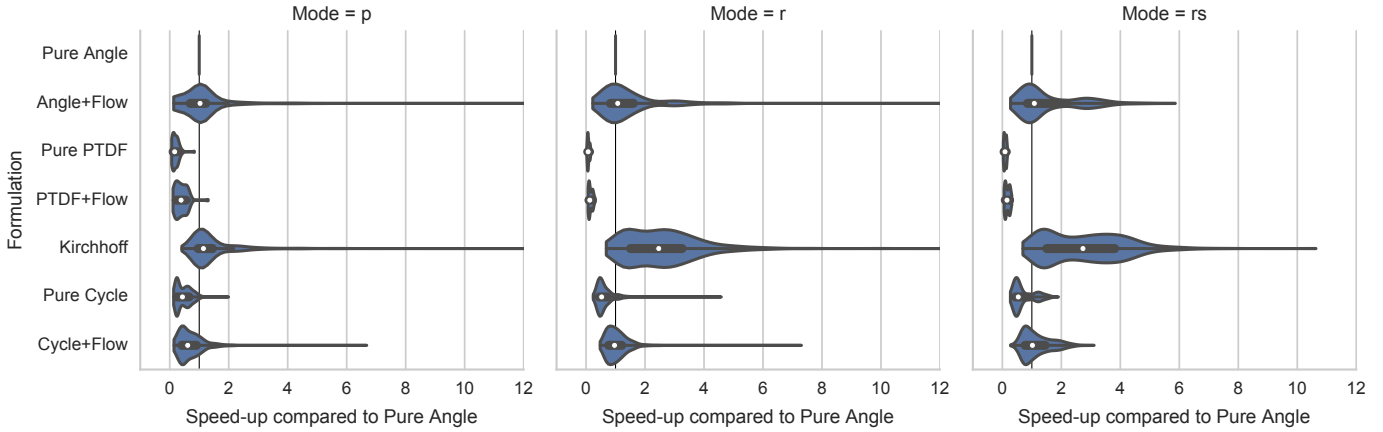


Figure 1: Speed-up of LOPF compared to Pure Angle for total time (read + pre-solve + solve). The violin plots give the distribution of speed-ups, while the box plots mark the 25% and 75% quantiles and the dot marks the median.

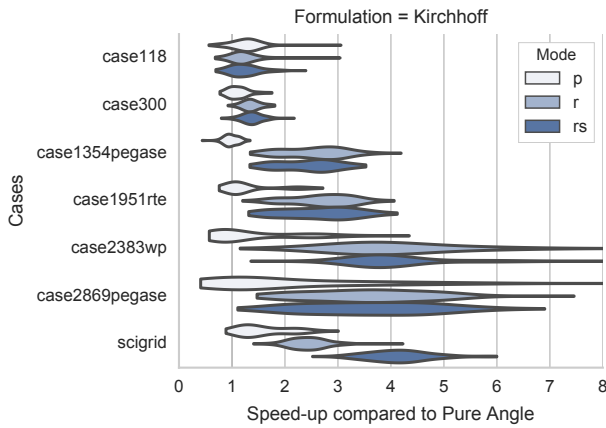


Figure 2: Kirchhoff LOPF speed-up compared to Pure Angle for total time (read + pre-solve + solve) per network case.

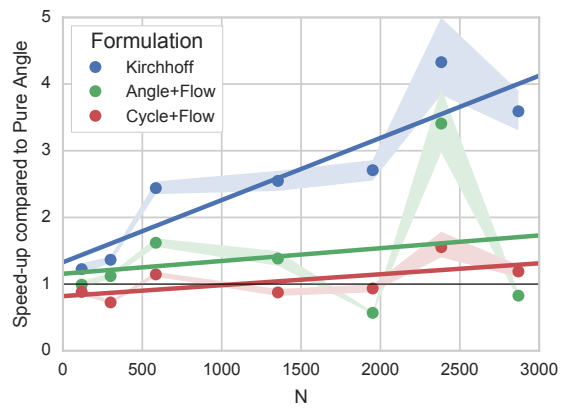


Figure 3: Speed-up of LOPF compared to Pure Angle per buses, shown are the mean values with 99% confidence interval and the result of a linear regression of all values for the three fastest formulations in mode 'r'.

some cases faster than the other methods, a result also reported by [16, 17].

5.3. Comparing specific speed-ups of the different formulations

The average speed-ups of the different formulations in the different modes masks considerable variations, both between the different network cases considered and within the instances for each case. Figure 1 shows violin plots of all the instances and all the cases for each mode and formulation combination, while in Figure 2 the different cases can be seen more clearly for the Kirchhoff formulation.

Take the speed-up of the Kirchhoff formulation in mode 'r' as an example. The average speed-up is 2.6, but this masks speed-ups for particular instances that range from a factor 0.7 (i.e. a 30% slow-down, for an instance of case118) to factor 20 (for an instance of case2383wp). Even within a particular case there is significant variation for particular instances, ranging for case2383wp from 1.2 up to 20, although with a strong clustering around the mean of 4.3.

In 3% of the instances the Kirchhoff formulation in mode 'r' is in fact slower than the Pure Angle formulation, and all these instances are for the cases with a smaller number of buses, case118 and case300. Figure 3 reveals that this is part of a bigger trend: In the 'r' mode, the Kirchhoff formulation speed-up grows with the size of the network, measured in terms of the number of buses. The increase in speed-up with network size also holds true for the 'rs' mode.

Of all the cases, instances and modes, the Kirchhoff formulation was fastest in 79.3% of the problems, while the Angle+Flow was fastest in 12.5%, Angle in 7.5% and Cycle+Flow in 0.7%. If we restrict to the modes 'r' and 'rs', then the Kirchhoff is fastest in 91.6% of the problems, Angle+Flow in 5.9%, Angle in 2.1% and Cycle+Flow in 0.4%.

The high level of variation of the speed-up for different cases and instances (reflecting different load and renewable profiles) means that in practice it may be advisable, given a particular problem, to run several formulations in parallel on a machine with multiple cores and take the solution from whichever solves first, much as linear program solvers like Gurobi can be config-

Table 4: Speed-up of LOPF with capacity optimization compared to the Pure Angle formulation, best formulation marked green

formulation	Mean solution time: Pure Angle [s]	Speed-up compared to Pure Angle			
		Angle+ Flow	Pure Kirchhoff	Pure Cycle	Cycle+ Flow
case118	1.00	0.89	1.15	0.74	0.84
case300	13.60	5.25	5.70	2.37	3.53
case1354pegase	539.93	3.01	12.97	2.05	4.76
case1951rte	914.55	3.10	9.39	1.73	4.36
case2383wp	7815.68	1.61	21.47	5.91	20.59
case2869pegase	5172.15	2.23	24.94	1.36	7.28
scigrd	347.72	2.73	10.04	3.97	10.26

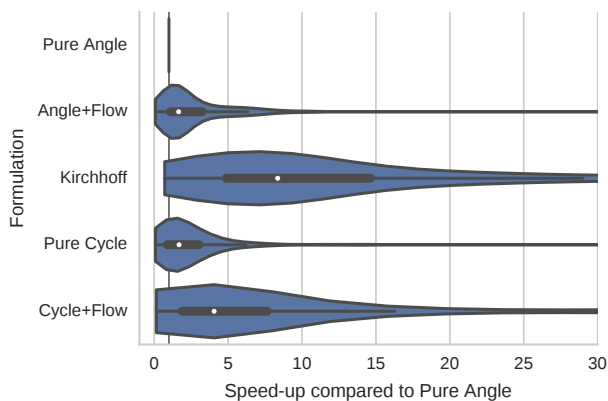


Figure 4: Speed-up of LOPF with capacity optimization compared to Pure Angle for total time (read + pre-solve + solve).

ured to run multiple solution algorithms in parallel, given the difficulty in predicting the runtime in advance.

5.4. Generation investment optimization

In a final set of computations, the capacities of all generators and storage units were included in the optimization following Section 4.2 for the case ‘rs’ with renewables and storage, optimized over 24 time periods. With capacity optimization, the problems take much longer to solve and a time-out of 10^4 seconds (just under 3 hours) was set on all calculations. In the Pure Angle formulation this limit was hit for some of the larger cases, breaching the limit in 55% of the instances for case2383wp and 18% of instances for case2869pegase. The PTDF method was excluded from this comparison given its slowness in previous results.

The results for the seven test cases are presented in Table 4 and graphed in Figure 4. Overall the speed-up factors are higher than for the LOPF without capacity optimization. Once again the Kirchhoff method is the fastest in most cases, averaging 12 times faster than Pure Angle over all cases, rising to 25 times faster for the biggest case case2869pegase. An individual instance of case1354pegase solved 213 times faster. The Cycle+Flow formulation performed better than it did for the LOPF without capacity optimization, solving on average 7.4 times faster than Pure Angle and faster than Angle+Flow in most cases. The Cycle+Flow formulation was on average the

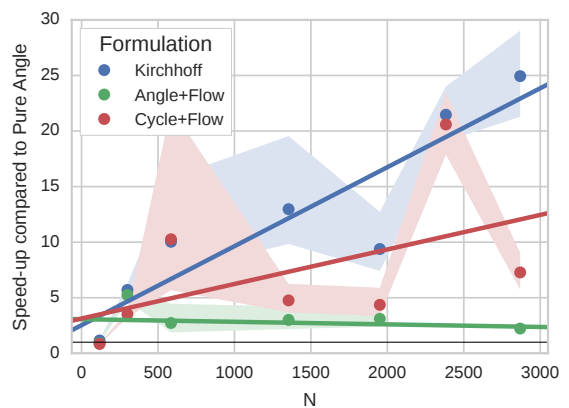


Figure 5: Speed-up of LOPF with capacity optimization compared to Pure Angle per buses. Shown are the mean values with 99% confidence interval and the result of a linear regression of all values.

fastest for the scigrd network, with an individual instance of the scigrd network finishing 388 times faster than Pure Angle.

Once again there is a trend for the speed-up to be higher with the Kirchhoff method the more nodes there are in the network, see Figure 5. This will benefit exactly the cases which take a long time to solve.

In these calculations only 24 time periods were included for the optimization. In general more periods are necessary to account for different weather conditions, which pushes computation times from hours to days. It is expected that the Kirchhoff method will thus make possible calculations that were not even possible with the Pure Angle formulation.

6. Conclusion

In this paper two new formulations of the linear optimal power flow (LOPF) problem, the Kirchhoff formulation and the Cycle formulation, have been presented and a comprehensive study of the numerical performance has been provided. The new formulations both use a graph-theoretic decomposition of the network into a spanning tree and closed cycles.

In one formulation, the Kirchhoff formulation, which implements the two Kirchhoff circuit laws directly on the flow variables, the LOPF is shown to perform considerably faster than the standard Angle formulation used in today’s power system

tools. It shows the greatest speed-up in very large networks with decentralized generation, which are exactly the kinds of problems that are becoming increasingly important with the rise of distributed renewable energy. In the Kirchhoff formulation the LOPF can solve up to 20 times faster for particular cases, while averaging a speed-up of approx. 3 for the networks considered in this paper. In 92% of the problems with distributed generation, the Kirchhoff formulation was the fastest formulation. If generation capacities are also optimized, the average speed-up rises to a factor of 12, reaching up to factor 213 in a particular instance. In a small number of specific cases the Cycle formulation was the fastest.

Future further applications could include the transmission expansion problem and the application of graph decomposition to the full non-linear optimal power flow problem.

Acknowledgments

We gratefully acknowledge support from the German Federal Ministry of Education and Research (BMBF grant nos. 03SF0472A-E) and the Helmholtz Association (joint initiative ‘Energy System 2050 – a contribution of the research field energy’ and grant no. VH-NG-1025 to D.W.). The work of H. R. was supported in part by the IMPRS Physics of Biological and Complex Systems, Göttingen.

References

- [1] F. Capitanescu, Critical review of recent advances and further developments needed in AC optimal power flow, *Electric Power Systems Research* 136 (2016) 57 – 68. doi:10.1016/j.epsr.2016.02.008.
- [2] K. Purchala, L. Meeus, D. V. Dommelen, R. Belmans, Usefulness of DC power flow for active power flow analysis, in: *IEEE Power Engineering Society General Meeting*, 2005, pp. 454–459 Vol. 1. doi:10.1109/PES.2005.1489581.
- [3] B. Stott, J. Jardim, O. Alsac, DC power flow revisited, *IEEE Trans. Power Syst.* 24 (3) (2009) 1290. doi:10.1109/TPWRS.2009.2021235.
- [4] F. C. Schweppe, M. C. Caramanis, R. D. Tabors, R. E. Bohn, *Spot Pricing of Electricity*, Norwell, MA: Kluwer, 1988.
- [5] B. Burstedde, *Essays on the economic of congestion management - theory and model-based analysis for Central Western Europe*, Ph.D. thesis, Universität zu Köln (2012).
- [6] A. J. Wood, B. F. Wollenberg, G. B. Sheblé, *Power Generation, Operation and Control*, John Wiley & Sons, New York, 2014.
- [7] F. Capitanescu, J. M. Ramos, P. Panciatici, D. Kirschen, A. M. Marcolini, L. Platbrood, L. Wehenkel, State-of-the-art, challenges, and future trends in security constrained optimal power flow, *Electric Power Systems Research* 81 (8) (2011) 1731 – 1741. doi:10.1016/j.epsr.2011.04.003.
- [8] G. Latorre, R. D. Cruz, J. M. Areiza, A. Villegas, Classification of publications and models on transmission expansion planning, *IEEE Trans. Power App. Syst.* 18 (2) (2003) 938–946. doi:10.1109/TPWRS.2003.8111683.
- [9] S. Lumbrales, A. Ramos, F. Banez-Chicharro, Optimal transmission network expansion planning in real-sized power systems with high renewable penetration, *Electric Power Systems Research* 149 (2017) 76 – 88. doi:10.1016/j.epsr.2017.04.020.
- [10] T. Pesch, H.-J. Allelein, J.-F. Hake, Impacts of the transformation of the german energy system on the transmission grid, *Eur. Phys. J. Special Topics* 223 (2014) 2561. doi:10.1140/epjst/e2014-02214-y.
- [11] A. J. Conejo, J. A. Aguado, Multi-area coordinated decentralized DC optimal power flow, *IEEE Transactions on Power Systems* 13 (4) (1998) 1272–1278. doi:10.1109/59.736264.
- [12] A. G. Bakirtzis, P. N. Biskas, A decentralized solution to the DC-OPF of interconnected power systems, *IEEE Transactions on Power Systems* 18 (3) (2003) 1007–1013. doi:10.1109/TPWRS.2003.814853.
- [13] O. Mgel, G. Andersson, J. L. Mathieu, Reducing the computational effort of stochastic multi-period DC optimal power flow with storage, in: *2016 Power Systems Computation Conference*, 2016, pp. 1–7. doi:10.1109/PSCC.2016.7541033.
- [14] H. Yamin, K. Al-Tallaq, S. Shahidehpour, New approach for dynamic optimal power flow using Benders decomposition in a deregulated power market, *Electric Power Systems Research* 65 (2) (2003) 101 – 107. doi:10.1016/S0378-7796(02)00224-9.
- [15] Y. Wang, S. Wang, L. Wu, Distributed optimization approaches for emerging power systems operation: A review, *Electric Power Systems Research* 144 (2017) 127 – 135. doi:10.1016/j.epsr.2016.11.025.
- [16] V. Hinojosa, J. Velsquez, Improving the mathematical formulation of security-constrained generation capacity expansion planning using power transmission distribution factors and line outage distribution factors, *Electric Power Systems Research* 140 (2016) 391 – 400. doi:10.1016/j.epsr.2016.06.002.
- [17] Stochastic security-constrained generation expansion planning based on linear distribution factors, *Electric Power Systems Research* 140 (2016) 139 – 146. doi:10.1016/j.epsr.2016.06.028.
- [18] A. Minot, Y. M. Lu, N. Li, A parallel primal-dual interior-point method for DC optimal power flow, in: *2016 Power Systems Computation Conference (PSCC)*, 2016, pp. 1–7. doi:10.1109/PSCC.2016.7540826.
- [19] J. J. Grainger, W. D. Stevenson Jr., *Power System Analysis*, McGraw-Hill, New York, 1994.
- [20] R. D. Zimmerman, C. E. Murillo-Sanchez, R. J. Thomas, *MATPOWER: Steady-state operations, planning and analysis tools for power systems research and education*, *IEEE Trans. Power Syst.* 26 (2011) 12. doi:10.1109/TPWRS.2010.2051168.
- [21] DIGSILENT GmbH, PowerFactory, <http://digsilent.de/> (2016).
- [22] PowerWorld Corporation, PowerWorld, <https://www.powerworld.com/> (2017).
- [23] F. Milano, An open source power system analysis toolbox, *IEEE Transactions on Power Systems* 20 (3) (2005) 1199–1206. doi:10.1109/TPWRS.2005.851911. URL <https://doi.org/10.1109/TPWRS.2005.851911>
- [24] H. Ronellenfisch, M. Timme, D. Witthaut, A dual method for computing power transfer distribution factors, *IEEE Trans. Power Syst.* 32 (2) (2016) 1007–1015. doi:10.1109/TPWRS.2016.2589464.
- [25] H. Ronellenfisch, D. Manik, J. Hörsch, T. Brown, D. Witthaut, Dual theory of transmission line outages, *IEEE Transactions on Power Systems* PP (99). arXiv:1606.07276, doi:10.1109/TPWRS.2017.2658022.
- [26] B. Kocuk, H. Jeon, S. S. Dey, J. Linderoth, J. Luedtke, X. A. Sun, A Cycle-Based Formulation and Valid Inequalities for DC Power Transmission Problems with Switching, *Operations Research* 64 (4) (2016) 922–938. doi:10.1287/opre.2015.1471.
- [27] R. Diestel, *Graph Theory*, Springer, New York, 2010.
- [28] M. E. J. Newman, *Networks – An Introduction*, Oxford University Press, Oxford, 2010.
- [29] P. Kundur, N. Balu, M. Lauby, *Power system stability and control*, EPRI power system engineering series, McGraw-Hill, 1994.
- [30] R. Lincoln, *PYPPOWER Version 5.0*, 2015. URL <https://github.com/rw1/PYPPOWER>
- [31] Hagspiel, S., Jägemann, C., Lindenburger, D., Brown, T., Cherevatskiy, S., Tröster, E., Cost-optimal power system extension under flow-based market coupling, *Energy* 66 (2014) 654–666.
- [32] J. A. Taylor, *Convex Optimization of Power Systems*, Cambridge University Press, 2015.
- [33] J. Morales, A. Conejo, H. Madsen, P. Pinson, M. Zugno, *Integrating Renewables in Electricity Markets: Operational Problems*, Springer, 2014.
- [34] A. Alqurashi, A. H. Etemadi, A. Khodaei, Treatment of uncertainty for next generation power systems: State-of-the-art in stochastic optimization, *Electric Power Systems Research* 141 (2016) 233 – 245. doi:10.1016/j.epsr.2016.08.009.
- [35] Deutsche Energie-Agentur, DENA-Netzstudie II, online at <http://www.dena.de/publikationen/energiesysteme> (2010).
- [36] Brown, T., Schierhorn, P., Tröster, E., Ackermann, T., Optimising the European transmission system for 77% renewable electricity by 2030, *IET Renewable Power Generation* 10 (1) (2016) 3–9.

- [37] T. Brown, J. Hrsch, D. Schlachtberger, Pypsa: Python for power system analysis, ArXiv e-prints arXiv:1707.09913.
URL <https://arxiv.org/abs/1707.09913>
- [38] Gurobi Optimization Inc., Gurobi optimizer reference manual (2016).
URL <http://www.gurobi.com>
- [39] C. Jozs, S. Fliscounakis, J. Maeght, P. Panciatici, Data in MATPOWER and QCQP Format: iTesla, RTE Snapshots, and PEGASE, ArXiv e-prints arXiv:1603.01533.
URL <https://arxiv.org/abs/1603.01533>
- [40] C. Matke, W. Medjroubi, D. Kleinhans, SciGRID - An Open Source Reference Model for the European Transmission Network (v0.2) (Jul. 2016).
URL <http://www.scigrid.de>
- [41] G. B. Andresen, A. A. Søndergaard, M. Greiner, Validation of danish wind time series from a new global renewable energy atlas for energy system analysis, *Energy* 93, Part 1 (2015) 1074 – 1088.
doi:<http://dx.doi.org/10.1016/j.energy.2015.09.071>.
- [42] J. Köster, S. Rahmann, Snakemake: a scalable bioinformatics workflow engine, *Bioinformatics* 28 (19) (2012) 2520.
doi:10.1093/bioinformatics/bts480.
- [43] T. Brown, J. Hrsch, D. Schlachtberger, Python for Power System Analysis (PyPSA) Website.
URL <https://pypsa.org/>